PHYSICAL REVIEW A VOLUME 24, NUMBER 3 SEPTEMBER 1981

Light-scattering studies of moderately dense gas mixtures: Hydrodynamic regime

L. Letamendia, J. P. Chabrat, G. Nouchi, J. Rouch, and C. Vaucamps
Centre de Physique Moleculaire Optique et Hertzienne, Universite de Bordeaux I, 351 Cours de la Liberation, 33405 Talence, France*

S.-H. Chen
Nuclear Engineering Department, Massachusetts Institute of Technology, Cambridge, Massachusetts 02139
(Received 6 November 1980)

Measurements of the Rayleigh-Brillouin spectra of light scattered by two classes of gaseous mixture; helium-xenon, and helium-hydrogen and helium-deuterium, have been performed over a range of density, concentration, and wave vectors. For He-Xe mixtures, under certain experimental conditions the data are accurately accounted for by a complete two-component hydrodynamic theory and light scattering has been shown to be a good method to deduce the thermal diffusion coefficient. We have thus determined in a quantitative way the range of applicability of the hydrodynamic theory. On the other hand, when the partial density of helium is not too small, systematic deviations between experimental and the calculated spectra are observed. These deviations can be understood in terms of kinetic effects to be discussed in a subsequent paper. For He-H_2 and He-D_2 mixtures, the hydrodynamic theory is in good agreement with our experimental data in the full range of densities and concentrations. We discuss the reason for this different behavior for the two classes of mixtures.

I. INTRODUCTION

The dynamic structure factor $S(q,\omega)$ of one-component rare-gas fluids has been extensively studied by light scattering[1] and coherent neutron scattering[2] during the last decade at different density and wave-vector ranges. While the neutron scattering measurements focused attention on high-density regions (higher than the critical density) and studied density fluctuations of wavelengths of the order of atomic size, the light-scattering experiments are generally confined to the dilute-gas regime where the wavelength of light ($\simeq$5000 Å) is of the order of interatomic distances. In this very low-density region (number density $\simeq 10^{19}$–10^{20} atoms/cm^3) it was found that the dynamic structure factors measured by light scattering agree well with predictions of the Boltzmann kinetic equation in both the kinetic ($ql > 1$, l = mean free path) and hydrodynamic ($ql < 1$) regime. Furthermore, the kinetic theory calculations,[3] and a recent experimental result of Ghaem-Maghami and May[1(e)] show that at low densities the dynamic structure factor in the kinetic regime is relatively insensitive to the interaction potential between atoms for rare gases at room temperature.

In a binary gaseous mixture, there are in general four parameters called Knudsen number Y_{ab} (Refs. 4) which characterize the nature of density fluctuations. The Knudsen number is proportional to the ratio of wavelength of actual fluctuations to wave-free path between collisions. We shall see below that for a given binary gas mixture experimental results can be classified by using two Knudsen numbers between collision of like pairs, namely,

$$Y_{ii} \simeq \frac{1}{ql_i}, \quad i = a \text{ or } b$$

where l_i is the mean free path between a like pair and is approximately given by $l_i = (\sqrt{2}\pi n_i \sigma_i^2)^{-1}$. n_i is the number density of particle i and σ_i the equivalent hard-sphere diameter. A kinetic behavior of the mixture is generally expected if Y_{aa} and Y_{bb} are both smaller than unity. On the other hand, a hydrodynamic behavior is expected if any one of Y_{aa} or Y_{bb} are much greater than unity.[4] In Fig. 1 we indicate in a two-parameter space (Y_{aa} vs Y_{bb}) regions where various experiments have been performed.

Relatively fewer experimental works have been reported for two-component rare-gas fluids. The earliest study of the He-Xe mixture up to 8 atm pressure was reported by Gornall and Wang.[5] They found that as an increasing amount of light impurity He is added to Xe gas initially at 8 atm, pronounced broadening and frequency pulling of the Brillouin components result. They attributed the effect to a strong hydrodynamic coupling between the sound wave and concentration diffusion in the mixture. In Fig. 1 their experiment is indicated by a black horizontal line denoted by A. Clark[6] extended the study of the He-Ne mixture into a nonhydrodynamic regime where Xe is dilute. Translational motion of Xe in helium was then modeled by a kinetic equation with a Fokker-Planck collision operator. Satisfactory agreement with light-scattering data was found. His experiment is indicated by a rectangular box B. More recently, Lao, Schoen, Chu, and Jackson[7] studied Rayleigh-Brillouin scattering in gaseous

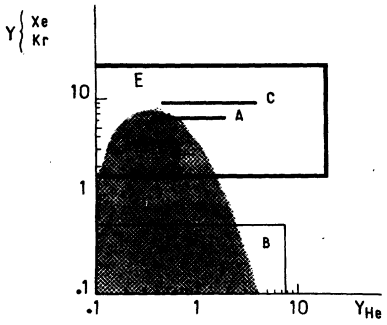

FIG. 1. A Y_{Xe} (or Y_{Kr}) vs Y_{He} parameter space which serves to identify the hydrodynamic and kinetic references. For the Xe-He mixture this experiment identified the shaded region to be the kinetic region while the rest of the space is hydrodynamic. According to Boley-Yip (Ref. 4) criteria the kinetic region is confined to $Y_{Xe} < 1$, $Y_{He} < 1$. Our experiment indicates that there is an extra region bounded by the shaded area and the box denoted by E where the kinetic description is definitely needed. Box E is the region where the present experiment is performed. Box B indicates Clark's experiment (Ref. 6) and C, A, D, respectively, represent experiments of Lao *et al.* (Ref. 7), Gornall and Wang (Ref. 5), and Bahardin *et al.* (Ref. 21).

mixtures of He-Kr and Ar-Kr up to pressures of 30 atm or so. Data were taken in the hydrodynamic regime and thus were compared with two-component hydrodynamic theory of Cohen *et al.*[8] Agreement was reported to be satisfactory. Their experiment is indicated by a horizontal line C.

In this series of papers we plan to present extensive studies of three gaseous binary mixtures: He-Xe, He-H_2, and He-D_2,[9] where the two-gas components are either of large difference in masses or of similar masses. Our experiments on He-Xe mixture cover a wide range of densities as indicated by a box E in Fig. 1. Although the He-Xe mixture has already been studied before, the experiments of Clark[6] were confined to a narrow domain where xenon is very dilute and its mean free path l_{Xe} is greater than q^{-1}, i.e., $Y_{Xe\text{-}Xe} < 1$. On the other hand, experiments of Gornall *et al.*,[5] were performed at high xenon density where $Y_{Xe} > 1$. As can be seen from Fig. 1, some of their results were obtained at rather low He density and high-q values leading to $Y_{He} < 1$. It is likely that some of their results would not show the hydrodynamic behavior. Besides, their spectra seem to be contaminated by a large amount of stray light. The more recent experiments on the mixture He-Kr by Lao *et al.*,[7] were performed in a regime expected to by hydrodynamic. However, the domain of Y values studied was very restricted and some stray light seems to be present also on their recording.

Use of a very stable and sensitive experimental setup involving frequency-stabilized high-power laser source, high-finesse Fabry-Perot interferometers and, most importantly, stray light-free scattering cells allows us to obtain a very accurate determination of the $S(q,\omega)$ profile. Then an extensive measurement of the structure factor covering a large domain of Y_{Xe} and Y_{He} values is of great interest in testing theoretical results on the Maxwell-model kinetic theory[4] and its limiting hydrodynamic[8] behavior in the He-Xe mixture.

In this first paper we mainly try to delineate the validity of hydrodynamic theory for the He-Xe mixture. In doing so we also identify a new region in the parameter space where kinetic description of the fluctuations is necessary. We shall emphasize the role played in the hydrodynamic regime by the coupling between temperature and concentration gradients via the thermal diffusion coefficient K_T. We shall then show that light scattering is a good tool to measure K_T in a large-mass-ratio binary mixture.

Dynamical studies of mixtures with mass ratio close to unity are also of interest. In this case it is known[10] that the thermal diffusion coefficient K_T is fairly small if the interparticle potential parameters of the two components are similar. This is the case of He-H_2 and He-D_2 mixtures (see Table I). When $K_T = 0$ the direct coupling between concentration and temperature fluctuations vanishes, leading to a great deal of simplification of hydrodynamic equations. Furthermore, at low densities the nonideality corrections to thermodynamic coefficients are small and these two systems can be used as a model system for testing the perfect-gas hydrodynamic behavior.

II. THEORETICAL BACKGROUND

In a light-scattering experiment from a fluid geometry of the experimental setup selects a Fourier component of thermal fluctuations of the local dielectric constant $\epsilon(\vec{r},t)$ with a wave vector $\vec{q}$ according to the relation

$$\vec{q} = \pm(\vec{k}_i - \vec{k}_s), \tag{1}$$

where $\vec{k}_i$ and $\vec{k}_s$ are the wave vectors of the incident and scattered light beams. In the case of Rayleigh-Brillouin scattering $|\vec{k}_i| \simeq |\vec{k}_s|$, and magnitude of the Bragg wave vector $\vec{q}$ is given by

$$|\vec{q}| \quad \frac{4\pi n}{\lambda} \sin\frac{\theta}{2}, \tag{2}$$

where λ, n, and θ are, respectively, the wavelength (in vacuum) of the laser beam, the index of refraction of the fluid, and the scattering angle.

The power spectral density $S(\vec{q},\omega)$ of the scat-

TABLE I. Atomic polarizabilities, Lennard-Jones parameters, and transport coefficients for the studied compounds.

	He	Xe	H_2	D_2
Polarizability α (10^{-24} cm^3)	0.204	3.999	0.82	0.82
(ϵ/k_B) (K)	10.12	299	33	39.3
σ in Å	2.576	4.055	2.968	2.948
η in 10^{-4} Poise	1.985	2.308	0.878	1.245
$pD_{\alpha\text{-He}}$ in $\frac{\text{cm}^2}{\text{sec}}$ atm		0.547	1.51	1.23

tered light is proportional to the Laplace-Fourier transform of the autocorrelation function of the fluctuations $\delta\epsilon(\vec{r},t)$, i.e.,

$$S(\vec{q},\omega)=2\,\mathrm{Re}\langle\delta\epsilon(\vec{q},\omega)\delta\epsilon(-\vec{q},0)\rangle\,, \tag{3}$$

where ω is the frequency shift in the scattering process. For a dilute gaseous mixture, $\epsilon(\vec{r},t)$ can be expressed in terms of atomic polarizabilities α_a and α_b and partial densities n_a and n_b of the two species using the Clausius-Mosotti equation

$$\epsilon(\vec{r},t)=1+4\pi[\alpha_a n_a(\vec{r},t)+\alpha_b n_b(\vec{r},t)]\,. \tag{4}$$

A simple calculation gives then the spectrum $S(\vec{q},\omega)$ in terms of the Laplace-Fourier transforms $S_{\alpha\beta}(\vec{q},\omega)$ $(\alpha,\beta=a,b)$ of the direct and cross-correlation functions of the partial density fluctuations δn_a and δn_b (Ref. 4):

$$S(\vec{q},\omega)=\frac{\alpha_a^2 n_a^0}{\alpha_a^2 n_a^0+\alpha_b^2 n_b^0}S_{aa}(q,\omega)+\frac{\alpha_b^2 n_b^0}{\alpha_a^2 n_a^0+\alpha_b^2 n_b^0}S_{bb}(q,\omega)$$

$$+\frac{2\alpha_a\alpha_b n_b^0}{\alpha_a^2 n_a^0+\alpha_b^2 n_b^0}S_{ba}(q,\omega)\,, \tag{5}$$

where n_a^0 and n_b^0 are the mean values of partial densities.

Boley and Yip[4] applied the method of the kinetic-model solution of the Boltzmann equation to calculate the partial density correlation functions $S_{\alpha\beta}(q,\omega)$ in a binary gaseous mixture of particles interacting via the Maxwell repulsive potential $V_{\alpha\beta}(\vec{r})=K_{\alpha\beta}/4r^4$, $K_{\alpha\beta}$ being the strength of the potential and r the distance between the two interacting particles. They have shown that in this case the spectra depend only on the following: (i) the mass ratio M_α/M_β; (ii) the scaled frequency $x_a=\omega/\sqrt{2}qv_a$; and (iii) the four Knudsen numbers $Y_{\alpha\beta}$ defined as

$$Y_{\alpha\alpha}=\frac{1.37n_\alpha^0(2K_\alpha/M_\alpha)^{1/2}}{\sqrt{2}qv_\alpha}\quad(\alpha=a,b)\,, \tag{6}$$

$$Y_{\alpha\beta}=\frac{n_\beta^0(K_{\alpha\beta}/M)^{1/2}}{\sqrt{2}qv_\alpha}\quad(\alpha=\beta,\beta=a,b)\,. \tag{7}$$

Here M_α is the mass of particle α, $v_\alpha=(k_BT/M_\alpha)^{1/2}$ the mean thermal speed of particle α, and $M=M_aM_b/(M_a+M_b)$ the reduced mass of the a-b pair.

Using the Maxwell model one can also express the force constant K_α in terms of shear viscosity η_α of the pure gas α and $K_{\alpha\beta}$ in terms of the mutual diffusion constant $D_{\alpha\beta}$. As a result we can then compute both $Y_{\alpha\alpha}$ and $Y_{\alpha\beta}$ using the formula

$$Y_{\alpha\alpha}=0.471\frac{P_\alpha}{qv_\alpha\eta_\alpha}\,, \tag{8}$$

$$Y_{\alpha\beta}=\left(\frac{1}{(2\times0.8122)^{1/2}}\right)\frac{k_BT}{Mv_\alpha q}\frac{P_\beta}{(pD_{\alpha\beta})}\,, \tag{9}$$

where p and p_α (or p_β) are, respectively, the total and partial pressures of the gas mixture.

From (8) and (9) and values of transport coefficients given in Table I we obtain, respectively, for the three mixtures

(Xe-He): $Y_{ab}=23.8Y_b$, $Y_{ba}=0.84Y_a$,

(D_2-He): $Y_{ab}=2.95Y_b$, $Y_{ba}=2.16Y_a$,

(H_2-He): $Y_{ab}=2.94Y_b$, $Y_{ba}=2.63Y_a$.

These relations show that for a given mixture it is sufficient to use only a pair of Y_a and Y_b to classify the nature of the density fluctuations.

The scaling variables $Y_{\alpha\beta}$ defined this way appear to be a useful guide in discussing whether thermal fluctuations obey the hydrodynamic equations or not. However, the criteria for hydrodynamic behavior are much more complicated in a binary fluid than in a one-component gas. In addition to the case where $Y_{\alpha\beta}$ are all larger than unity, there are other possibilities which have been discussed by Boley and Yip as leading also to hydrodynamic behavior (Table I of Ref. 4).

Theories for the spectrum of light scattered from a binary mixture in the hydrodynamic regime have been formulated by Mountain and Deutch[11] and, more recently, corrected versions have been given by Cohen *et al.*,[8] and Lekkerkerker and Laidlaw.[12] The expression (5) of the spectrum is valid both in the kinetic and hydrodynamic regimes, but a more suitable set of variables in the hydrodynamic regime is the local fluctuations of three statistically independent thermodynamic variables: pressure $\delta p(\vec{r},t)$, concentration $\delta c(\vec{r},t)$, and $\delta\phi(\vec{r},t)=\delta T(\vec{r},t)-(T_0\alpha_T/\rho_0C_P)\delta p(\vec{r},t)$.

T_0, ρ_0 are the equilibrium values of temperature and mass density, C_P and α_T are, respectively, the specific heat and the thermal expansion coefficient at constant pressure, and $\delta T(\vec{r},t)$ the local temperature fluctuation.

Using the total mass density $\rho = M_a n_a + M_b n_b$ and the concentration $c = M_a n_a/\rho$, one can rewrite (4) as

$$\epsilon = 1 + 4\pi\rho\left(c\frac{\alpha_a}{M_a} + (1-c)\frac{\alpha_b}{M_b}\right). \tag{10}$$

The total density ρ is a function of the three thermodynamic variables p, ϕ, and c. One finds, by Taylor expansion, the local fluctuation of the dielectric constant which has the following expression:

$$\delta\epsilon(\vec{r},t) = \left(\frac{\delta\epsilon}{\delta\rho}\right)_c\left[\left(\frac{\delta\rho}{\delta\phi}\right)_{p,c}\delta\phi(\vec{r},t) + \left(\frac{\delta\rho}{\delta p}\right)_{\phi,c}\delta p(\vec{r},t)\right] + \left[\left(\frac{\delta\epsilon}{\delta c}\right)_\rho + \left(\frac{\delta\epsilon}{\delta\rho}\right)_\phi\left(\frac{\delta\rho}{\delta c}\right)_{\phi,p}\right]\delta c(\vec{r},t) = \sum_{i=1}^{3}\left(\frac{\delta\epsilon}{\delta X_i}\right)\delta X_i\,, \tag{11}$$

where

$$\left(\frac{\delta\epsilon}{\delta\rho}\right)_c = \frac{\epsilon-1}{\rho_0}\,,\quad \left(\frac{\delta\epsilon}{\delta c}\right)_\rho = 4\pi\rho_0\left(\frac{\alpha_a}{M_a} - \frac{\alpha_b}{M_b}\right),$$

$$\left(\frac{\delta\rho}{\delta\phi}\right)_{p,c} = \alpha_T\rho_0\,,\quad \left(\frac{\delta\rho}{\delta p}\right)_{\phi,c} = X_s\rho_0\,,\quad \left(\frac{\delta\rho}{\delta c}\right)_{\phi,p} = -\rho_0^2\left(\frac{\delta\mu}{\delta P}\right)_{T,c}.$$

χ_s and μ, respectively, are the adiabatic compressibility and the chemical potential.

In terms of the new set of variables the spectrum of scattered light is given by a sum of nine terms:

$$S(q,\omega) \simeq 2\,\mathrm{Re}\sum_{i,j=1}^{3}\left(\frac{\delta\epsilon}{\delta X_i}\right)\left(\frac{\delta\epsilon}{\delta X_j}\right)F_{ij}(q,i\omega)\langle|\delta X_j|^2\rangle\,, \tag{12}$$

where the X_j are the variables p, c, ϕ, $\langle|\delta X_j|^2\rangle$ their mean-square fluctuations, and $F_{ij}(a,i\omega)$ the Fourier-Laplace transform of the normalized correlation function of the fluctuating variables X_i and X_j.

In the hydrodynamic regime, the three δX_i together with the local longitudinal velocity $v(\vec{r},t)$ form a complete set of variables which obeys the four linearized hydrodynamic equations (density, concentration, energy, and longitudinal momentum conservation equations). The $F_{ij}(q,i\omega)$ are then the ij elements of the inverted hydrodynamic matrix. Detailed expressions of both 4×4 hydrodynamic matrix $M(q,i\omega)$ and approximate eigenvalues of it can be found in Ref. 8.

In the case of a gaseous mixture where the sound frequency is not much greater than the dissipation rates of heat and concentration fluctuations, the normal frequencies given by solution of the dispersion equation $\det|M(q,i\omega)| = 0$ depend strongly on couplings between the sound, thermal diffusion, and mass diffusion modes. Then approximate solutions of the dispersion equation given by Cohen *et al.*,[8] and Lekkerkerker and Laidlaw[12] are no longer valid and a complete solution has to be performed. The Rayleigh-Brillouin spectrum is then the weighted sum of three direct correlation functions ($pp, cc, \phi\phi$) and the three cross-correlation functions ($pc, p\phi, c\phi$). Each term involves the four normal modes of the system. The cross terms have a zero contribution to the total integrated intensity owing to the statistical independence of the variables at initial time.

An accurate numerical calculation of $S(q,\omega)$ requires a precise knowledge of both thermodynamic and transport coefficients. Inspection of the hydrodynamic matrix in Ref. 8 reveals that the two most important thermodynamic coefficients are specific heat ratio γ and $(\delta\mu/\delta c)_{p,T}$. The former depends essentially on the first- and second-order temperature derivatives of the second virial coefficient while the latter depends on the virial coefficient itself. These quantities can be calculated for a Lennard-Jones (LJ) gas mixture according to procedures given in Hirschfelder, Curtiss, and Bird.[10] As for the transport coefficients D_T, D_{12}, and η most of them have been measured with good precision for noble gas mixtures in the temperature and pressure range of this experiment. When experimental data are not available we use the Chapnann-Enskog expressions for the LJ gas mixture.[9,10]

III. EXPERIMENTALS

The setup for the Brillouin scattering experiment is schematically depicted in Fig. 2. A beam from a stabilized single-mode argon-ion laser (Spectra Physics Model 171) operating at 5145 Å with a power of 800 MW is focused by a lens L_1 into a high-pressure scattering cell C. This cell was designed by Dr. Cazabat[1(b)] previously for studying light scattering from very-low-pressure gases which require an extremely low stray light coming from the interior of the cell. The cell is made with a brass body and consists of four long arms each with a length of about 20 cm (volume $\simeq 0.5$ L) closed at the ends by coated high-pressure quartz windows. Inside the cell there are two apertures to further limit stray light from entering the scattered direction. Each cell is designed for a specific scattering angle θ and its complement $\pi - \theta$. During the course of the experiment, four cells are used which allow selection of the scattering angles: 30°, 45°, 60°, 90°, 120°, 130°, and 150° with the wave vector q ranging from 0.6×10^5 cm^{-1} to 3.0×10^5 cm^{-1}.

The scattering cell is filled with high-grade gases supplied by Societe Air-Liquide using high-

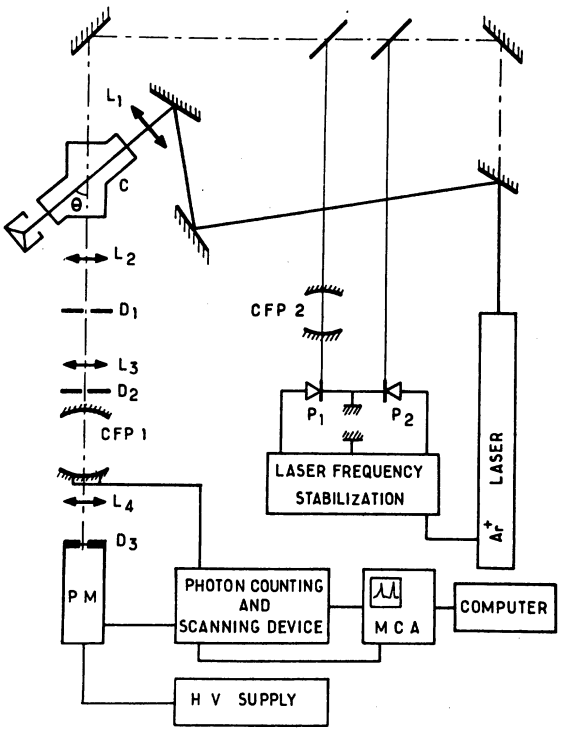

FIG. 2. Schematic diagram of the Rayleigh-Brillouin scattering setup. A crucial item for the present experiment is the stray light free cell C.

pressure handling equipment described by Veldkamp.[9] Partial pressure of the heavier component and the total pressure of the mixture are measured with either a pressure-voltage calibrated transducer or a Bourdon gauge. Molar composition of the sample is computed from the virial equation of state of a Lennard-Jones mixture. Potential parameters used for various gases are given in Table I.

The scattered light is focused onto a pinhole D_1 by a lens L_2 and the pinhole is then imaged by a lens L_3 onto the center of a confocal Fabry-Perot interferometer (CFP 1) through a limiting aperture D_2 of 1 mm. The CFP 1 has a finesse of about 50 and a spacing of 5.41 cm which can be piezoelectrically scanned. The outgoing beam from CFP 1 is then focused by a lens L_4 onto a pinhole D_3 lying in front of a low dark counts EMI 6256 S Phototube (PM). The photocounts are processed by a photon discriminator and fed into a 1024 channel analyzer (MCA) which stores and displays the data. The CFP 1 and MCA memory advance are synchronously scanned with a 1000 steps step-by-step ramp generator.

The response of the piezoelectric transducer in the CFP 2 has to be corrected for nonlinearity: for this purpose, the profile of the voltage sawtooth used for sweeping the transducer is made cubic in time. The linearity of the scanned frequency versus time is then better than 0.5%. Accurate measurements of the spectra require an instrumental line width of less than 30 MHz. Acoustic noise arising principally from cooling water of the laser tube produces frequency jitter greater than 30 MHz and furthermore, sometimes the lasing mode jumps. In order to stabilize the laser frequency, the following device has been used: two pin photodiodes P_1 and P_2 receive, respectively, a part of direct light from the laser and a part of laser beam which goes through a temperature controlled ($\pm 0.01°$ C) confocal Fabry-Perot (FP) interferometer CFP 2. The two signals are fed into a difference amplifier followed by a high-voltage amplifier, and output of the latter is then applied to a piezoelectric transducer attached to the back mirror of the laser. This serves to lock the laser frequency to the CFP 2 cavity frequency. Furthermore, the very slow thermal drift of the laser frequency is corrected for by a temperature control of the optical length of the laser cavity. The jitter of the laser output frequency is then reduced to less than 3 MHz during a period of several hours.

The combined laser and Fabry-Perot instrumental profile is then measured by recording light scattered from a dilute solution of polystyrene spheres. The true linewidth of the spectrum lies in the kHz domain and was checked by using light beating spectroscopy. The combined instrumental profile has been accurately fitted to an Airy function with a linewidth of 20 MHz [full width at half maximum (FWHM)].

In the case of He-Xe mixtures at high-He density and also for the He-D_2 and He-H_2 mixtures, a high-finesse (greater than 60) Tropel piezoelectrically scanned plane FP interferometer has been used.

In order to maintain the stability, all "optical parts" of the instrumental setup are tightened on a large (2.2 m × 1.4 m) granite table which is isolated from acoustic noise of the building.

Recordings of the light coming from an empty scattering cell show a flat background coming from thermal noise of the detector ($\simeq 5$ counts s^{-1}) alone and *no* peak at the laser frequency is observed. This assures us that the data are not contaminated by stray light. This, however, is not the case of all experiments previously reported.[5-7] Therefore, in our case, comparison of the experimental data to the theory needs only one normalization parameter which can be either the integrated intensity of the spectrum $S(q,\omega)$, or, more conveniently, the peak height of one of the Brillouin lines.

IV. EXPERIMENTAL RESULTS

Three binary mixtures have been studied: Xe-He, D_2-He, and H_2-He, at various total pressures and compositions. The choice of the constituents was made with consideration of obtaining a large range of variation of the atomic mass ratio: $M_{Xe}/M_{He}=33$; $M_{D_2}/M_{He}=1$; $M_{H_2}/M_{He}=0.5$. This parameter plays an important role in determining the dynamics of concentration and pressure fluctuations in a mixture as will be discussed in Sec. V.

In this paper we mainly discuss results obtained under conditions where parameter Y_{11} of Xe (or D_2 or H_2) is always greater than unity. It should be noted that the spectra are "hydrodynamic" for all pure Xe, H_2, and D_2 at the start of a series of experiments in the full range of pressure and wave vector used.

Table II summarizes all thermodynamic states where measurements were made for the Xe-He system. Partial pressure of xenon ranges from 1.82 to 8.5 atm while partial pressure of He was varied from zero to a maximum of 26 atm. Temperature was uniformly at 293 K. All four Knudsen numbers were calculated according to Eqs. (8) and (9). X_{Xe} denotes mole fraction of xenon gas in the mixture, θ the scattered angle, and H and NH indicate, respectively, that the spectrum is well fitted with hydrodynamic theory or not.

Measured spectra and their comparison with hydrodynamic calculations for most of the thermodynamic states listed in Table II are given successively in Figs. 3–7. Experimental results are indicated by dots and theoretical results by solid lines. Based on these figures and the last column in Table II, a nonhydrodynamic region in the Y_{Xe}-Y_{He} parameter space is constructed. It is the shaded parabolic region contained in the rectangular region denoted by E where all our experimental data lie.

Table III summarizes all the data available for H_2-He and D_2-He systems. It is to be noted that every one of the spectra is well fitted by the hydrodynamical theory. No kinetic region is found within the Y range explored by our experiments. The corresponding spectra and their comparison with hydrodynamic calculations are given in Fig. 8 for H_2-He and Fig. 9 for D_2-He mixtures.

V. DISCUSSION

A. Xe-He binary mixture

1. Validity of the hydrodynamic equations

In this paper we shall mainly discuss results obtained under conditions where parameter $Y_{11}\equiv Y_{Xe}$ is always greater than unity. This means initial partial pressures of Xe gas are all greater than 1 atm. Experiments were done with increasing He partial pressures from 0 to 100 atm (Ref. 9) which correspond to changing $Y_{22}\equiv Y_{He}$ from 1 to 20. Table I contains only part of the results for which the partial pressure of He is up to 26 atm. We are interested in detecting deviations from the hydrodynamic behavior at smaller values of Y_{He} depending on the initial magnitude of Y_{Xe}. Inspection of Figs. 3–7 shows that the pure Xe spectra in the beginning of each graph always show a well-structured Rayleigh-Brillouin triplet indicating the hydrodynamic behavior. As soon as some amounts of the He are added the Brillouin lines become strongly damped and seem to disappear at higher He mole fraction. Furthermore, Figs. 3–7 show that for a given amount of xenon gas there is an intermediate range of helium concentration where the spectra deviate substantially from hydrodynamic calculations. The deviation from hydrodynamic behavior is characterized by an appearance that the experimental spectra are more structured than the hydrodynamic prediction. The damping of Brillouin peaks, as an increasing amount of the light impurity He is added, can be understood qualitatively in the nonhydrodynamic regime as follows. The Brillouin components in Xe-He mixtures largely represent sound-wave propagation in xenon gas because of a peculiarity of very large polarizability of xenon atoms as compared to He atoms. Sound-wave propagation represents a collective oscillation of xenon atoms as a result of collisions among them. Addition of impurity atoms disrupts collisions between xenon atoms and hence the sound propagation in them. Light impurity atoms are most effective in these disruptive collisions because their thermal speeds are large. We shall discuss this aspect of the problem more quantitatively in the next paper. In the hydrodynamic regime where one does not talk in terms of the partial structure factor $S_{Xe\text{-}Xe}(q,\omega)$ (see Sec. II), one can explain the damping of sound in terms of an increased strength of coupling depends strongly on a parameter in the hydrodynamic matrix which is $D_{12}K_T^2(\partial\mu/\partial c)_{\rho,T}$. As we shall explain later in subsection B that for a binary mixture where mass ratio of the atoms is large, the thermodynamic derivative $(\partial\mu/\partial c)_{\rho,T}$ is proportional to the mass ratio. This is the case for the Xe-He mixture.

Experimental data on viscosity,[13] thermal conductivity,[14] thermal diffusion,[15] and mutual diffusion coefficients[22] are available for this mixture at some compositions. These results are used to calculate the best values of the LJ potential parameters ϵ and σ as listed in Table I. This set of

TABLE II. Calculated values of the 4 Knudsen parameters Y_{ab} for the He-Xe mixture at different pressures, compositions, and scattering angles ($\theta = 90°$ and $\theta = 30°$). The last column indicates whether the hydrodynamic theory agrees (*H*) or disagrees (*NH*) with the experimental results.

Helium-xenon mixture								
P_{Xe} (atm)	P_{He} (atm)	Y_{Xe}	Y_{He}	$Y_{Xe\text{-}He}$	$Y_{He\text{-}Xe}$	X_{Xe}	θ	
1.82	0	1.635	Pure	Xenon	1.377	1.0	90	*H*
1.82	0.39	1.635	0.071	1.688	1.377	0.82	90	*NH*
1.82	2.65	1.635	0.474	11.44	1.377	0.40	90	*NH*
1.82	5.95	1.635	1.079	25.76	1.377	0.237	90	*H*
1.82	9.40	1.635	1.711	40.64	1.377	0.16	90	*H*
1.82	25.94	1.635	4.715	112.3	1.377	0.067	90	*H*
3.75	0	3.363	Pure	Xenon		1.0	90	*H*
3.75	0.56	3.363	0.094	2.424	2.833	0.87	90	*NH*
3.75	1.81	3.363	0.329	7.83	2.833	0.68	90	*NH*
3.75	3.51	3.363	0.638	15.19	2.833	0.52	90	*NH*
3.75	6.45	3.363	1.173	27.9	2.833	0.37	90	*NH*
3.75	11.78	3.363	2.142	50.96	2.833	0.24	90	*H*
3.75	21.5	3.363	3.91	93	2.833	0.15	90	*H*
5.97	0	5.353	Pure	Xenon		1.0	90	*H*
5.97	0.57	5.353	0.104	2.466	4.195	0.91	90	*NH*
5.97	1.25	5.353	0.227	5.409	4.195	0.83	90	*NH*
5.97	3.8	5.353	0.691	16.44	4.195	0.62	90	*NH*
5.97	4.17	5.353	0.758	18.04	4.195	0.599	90	*NH*
5.97	9.17	5.353	1.667	39.68	4.195	0.40	90	*H*
7.32	0	6.564	Pure	Xenon		1	90	*H*
7.32	1.59	6.564	0.289	6.882	5.531	0.82	90	*NH*
7.32	3.28	6.564	0.596	14.19	5.531	0.69	90	*NH*
7.32	7.14	6.564	1.298	30.89	5.531	0.52	90	*NH*
7.32	10.42	6.564	1.894	45.09	5.531	0.42	90	*H*
7.32	13.14	6.564	2.382	56.86	5.531	0.37	90	*H*
6.47	0	15.83	Pure	Xenon		1.0	30	*H*
6.47	2.20	15.83	1.092	25.99	13.340	0.753	30	*H*
6.47	3.85	15.83	1.912	45.48	13.340	0.63	30	*H*
2.66	0	6.51	Pure	Xenon		1.0	30	*H*
2.66	1.11	6.51	0.551	13.11	5.487	0.7	30	*NH*
2.66	6.9	6.51	3.426	84.16	5.487	0.28	30	*H*
8.5	0	20.81	Pure	Xenon		1.0	30	*H*
8.5	4.0	20.81	1.986	47.26	17.34	0.68	30	*H*
8.5	4.99	20.81	2.482	58.96	17.34	0.64	30	*H*
8.5	5.4	20.81	2.680	63.80	17.34	0.62	30	*H*
8.5	6.2	20.81	3.029	71.70	17.34	0.59	30	*H*
8.5	6.8	20.81	3.377	80.35	17.34	0.57	30	*H*

parameters are then used to compute transport coefficients for the actual experimental conditions. Likewise we can use the parameters to calculate the second-order virial coefficient and thus also the nonideality corrections to the thermodynamic coefficients. At the largest Xe density, these corrections can reach as much as 7% especially for compressibilities and specific heat ratio.

The "theoretical" hydrodynamic spectra are then convoluted with the instrumental profile for comparison with experiments. They are shown as solid lines in Figs. 3–7. Good agreements are observed for two ranges of concentrations: (i) at very low molar fraction of He ($X_{He} < 0.05$). These spectra are not shown because there is no significant departure from spectra of pure Xe; (ii) at molar fractions of He higher than a "critical" value which depends on the partial pressure of Xe. For example, at $P_{Xe} = 7.32$ atm the "initial" value of the He mole fraction is $X_{He} = 0.55$. In Fig. 1 we show in the Y_{Xe}-Y_{He} parameter space where the hydrodynamic behavior is not observed by a shaded region. The points of discussion above correspond to the shaded region above the

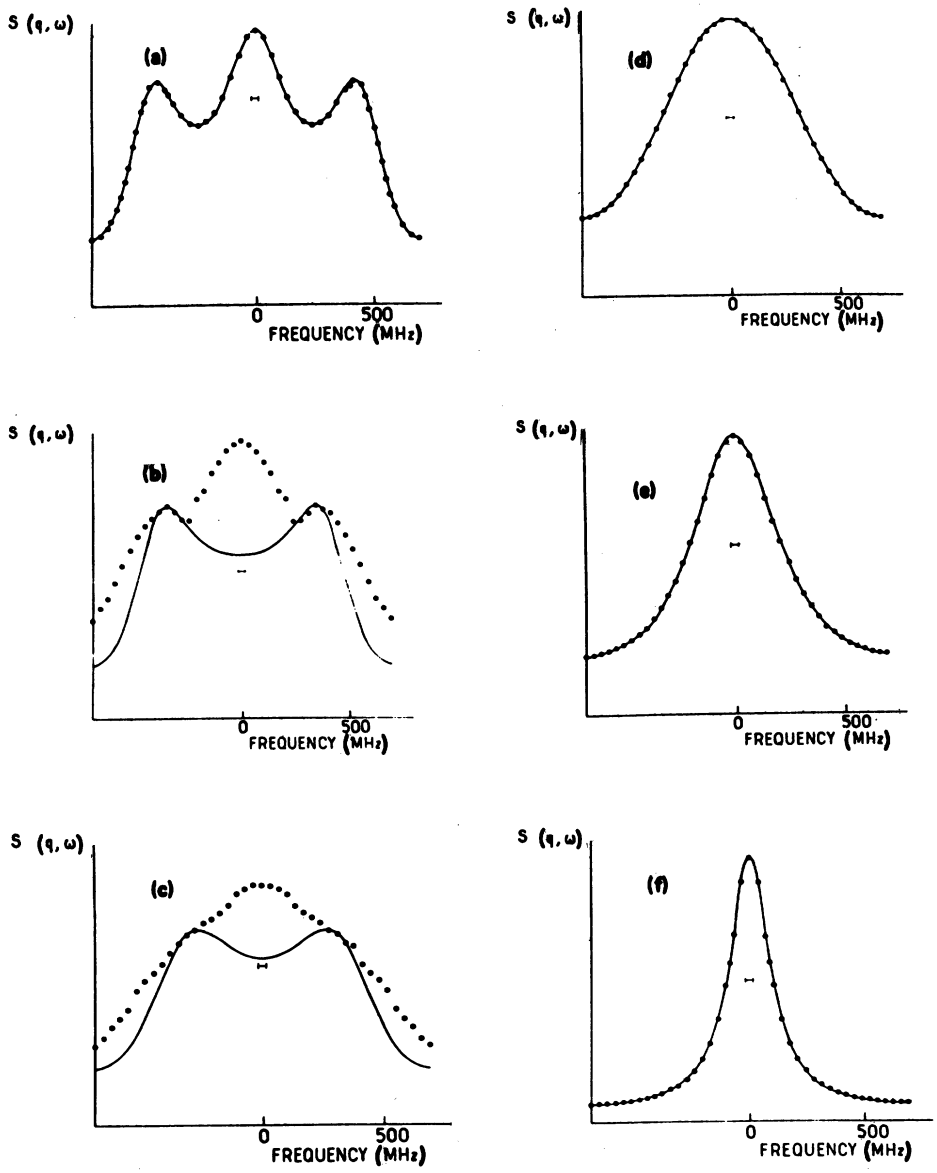

FIG. 3. Rayleigh-Brillouin spectra of He-Xe mixtures. Dots are experimental points and solid lines are results of hydrodynamic calculations as described in Sec. II. All spectra are taken at $T = 293$ K. Each curve refers to different gas compositions, but all taken at the same $q = 1.725 \times 10^5$ cm^{-1} and $P_{Xe} = 1.82$ atm. (a) $P_{He} = 0$ atm; (b) $P_{He} = 0.39$ atm; (c) $P_{He} = 2.65$ atm; (d) $P_{He} = 5.93$; (e) $P_{He} = 9.4$ atm; (f) $P_{He} = 25.94$ atm. The small bar in the center of each graph represents the combined frequency resolution of the spectrometer.

horizontal line $Y_{Xe} = 1.6$.

For the range of experimental conditions we have in Xe-He mixture, Boley and Yip[4] gave criteria for validity of the hydrodynamic description. They are

(a) All Y_{Xe}, Y_{He}, $Y_{Xe\text{-}He}$, $Y_{He\text{-}Xe} > 1$,

(b) $Y_{Xe} > 1$, $Y_{Xe\text{-}He} > 1$, $Y_{He\text{-}Xe} > 1$, $Y_{He} < 1$.

From Table I we see the criterion (a) is certainly valid. However, the criterion (b) is clearly not obeyed by our data. Possible reasons for failure of the criterion (b) are that K_T is appreciably different from zero in the Xe-He mixture; and that at higher densities the nonideality corrections for the thermodynamic coefficients are important. Boley and Yip solved the Boltzmann equation for the Maxwell-model potential which is known to be consistent only to the perfect-gas behavior for its equilibrium properties and it predicts K_T which is identically zero.

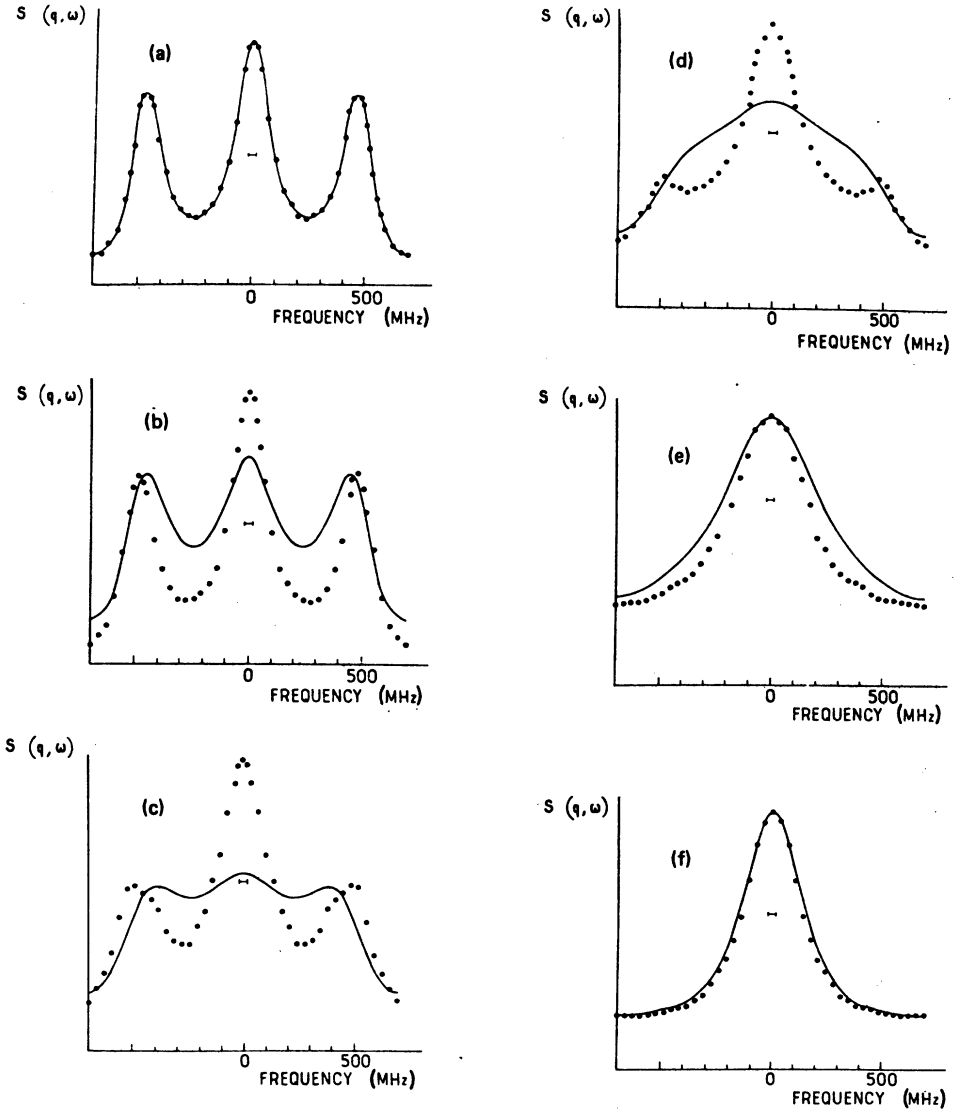

FIG. 4. Rayleigh-Brillouin spectra of He-Xe mixtures at $q = 1.727 \times 10^5$ cm^{-1} and $P_{Xe} = 3.75$ atm. (a) $P_{He} = 0$ atm; (b) $P_{He} = 0.56$ atm; The dotted line represents experimental data. The solid line represents hydrodynamic calculation. See Fig. 3 for additional legend.

2. *Thermal diffusion coefficient*

In order to test the sensitivity of light-scattering spectra to the value of K_T we compute theoretical spectra for different values of K_T. We show in Fig. 10 one such result for $P_{Xe} = 5.97$ atm and $P_{He} = 3.78$ atm which corresponds to $Y_{Xe} = 5.76$ and $Y_{He} = 1.14$. There is a good agreement between experimental data and the theory for $K_T = 0.321$ which is a value inferred from experimental data of Saviron *et al.*,[15] on K_T. This value also agrees with the kinetic-theory result computed with the LJ parameters of the Xe-He mixture to a few percent. We give in Table V the values of integrated intensities A_1 and A_2 and linewidth Γ_1 and Γ_2 of the two central modes for $K_T = 0.321$ and $K_T = 0$ (corresponding to the Maxwell model).[10] Label 1 refers to the broader line. As K_T is increased from zero the net result is an interchange of intensities between lines 1 and 2 resulting in sharpening of the central line. On the other hand, the integrated intensity of the Brillouin line remains almost unchanged (e.g., term B of Table V) whereas its width decreases significantly and its center shifted

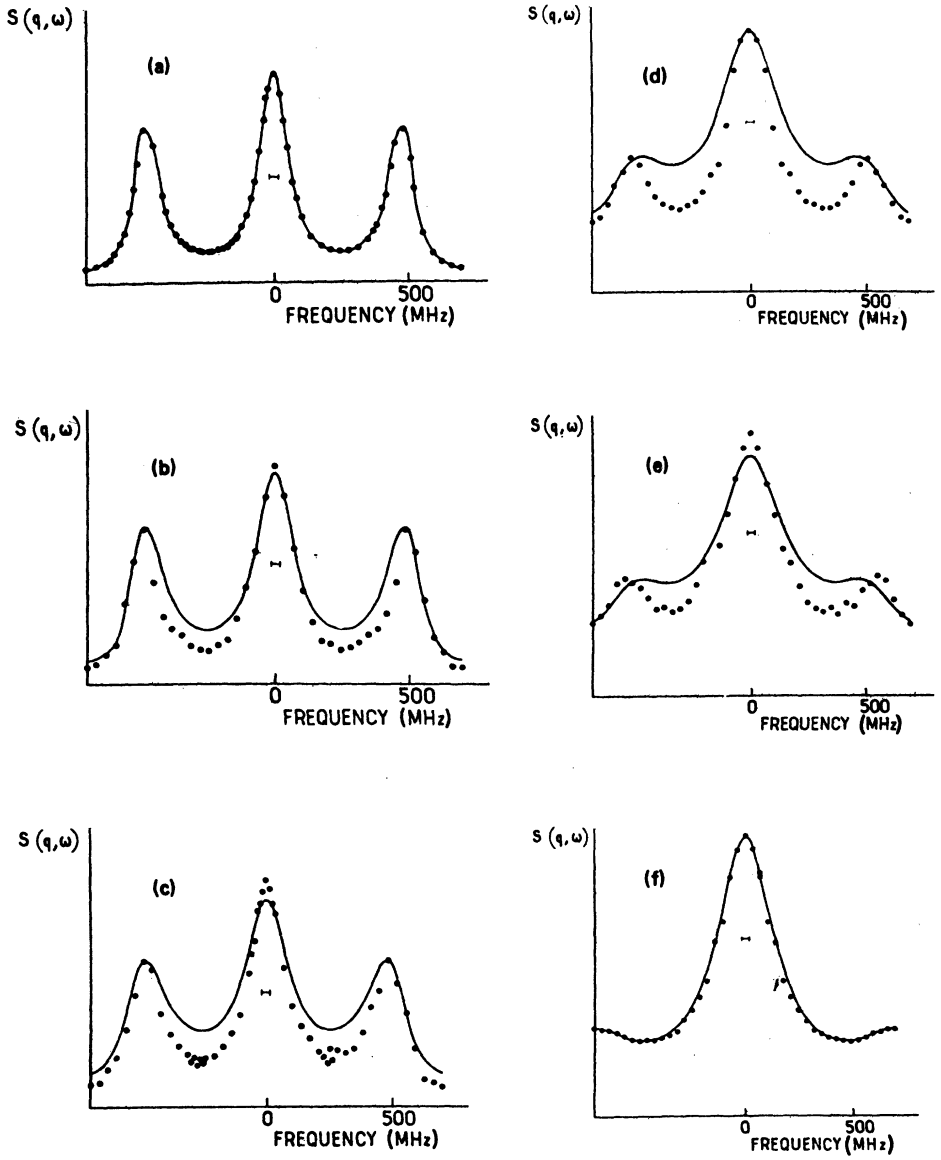

FIG. 5. Rayleigh-Brillouin Spectra of He-Xe mixtures at $q = 1.727 \times 10^5$ cm^{-1} and $P_{Xe} = 5.97$ atm. (a) $P_{He} = 0$ atm; (b) $P_{He} = 0.56$ atm; (c) $P_{He} = 1.24$ atm; (d) $P_{He} = 3.80$ atm; (e) $P_{He} = 4.16$ atm; (f) $P_{He} = 9.17$ atm. See Fig. 3 for additional legend.

to higher frequency.

In order to explain the sensitivity of the calculated spectra to the value of K_T, let us come back to the hydrodynamic equations. From Onsager symmetry laws, the heat flux $\vec{J}_q$ is coupled to the concentration gradient grad c of the component 1 by the coefficient[16]

$$-\rho_0 D_{12} K_T \left(\frac{\partial \mu}{\partial c}\right)_{T,P},$$

whereas the mass flux of 1 is coupled to grad δT via a coefficient

$$-\rho_0 D_{12} \frac{K_T}{T_0}.$$

The coupling parameter between the two central modes, $\delta = (K_T^2/T_0 C_P)(\partial \mu/\partial c)_{T,P}$, vanishes when $K_T = 0$, thus removing the coupling and the frequencies become, respectively, $\Gamma_1 = D_T q^2$, $\Gamma_2 = D_{12} q^2$. Furthermore, we observe that when $K_T \neq 0$ the associated thermodynamic coefficient $(\partial \mu/\partial c)_{T,P}$ becomes relevant. This coefficient has a strong dependence on the mass ratio M_1/M_2 as it can be seen from the expression of $(\partial \mu/\partial c)_{T,P}$

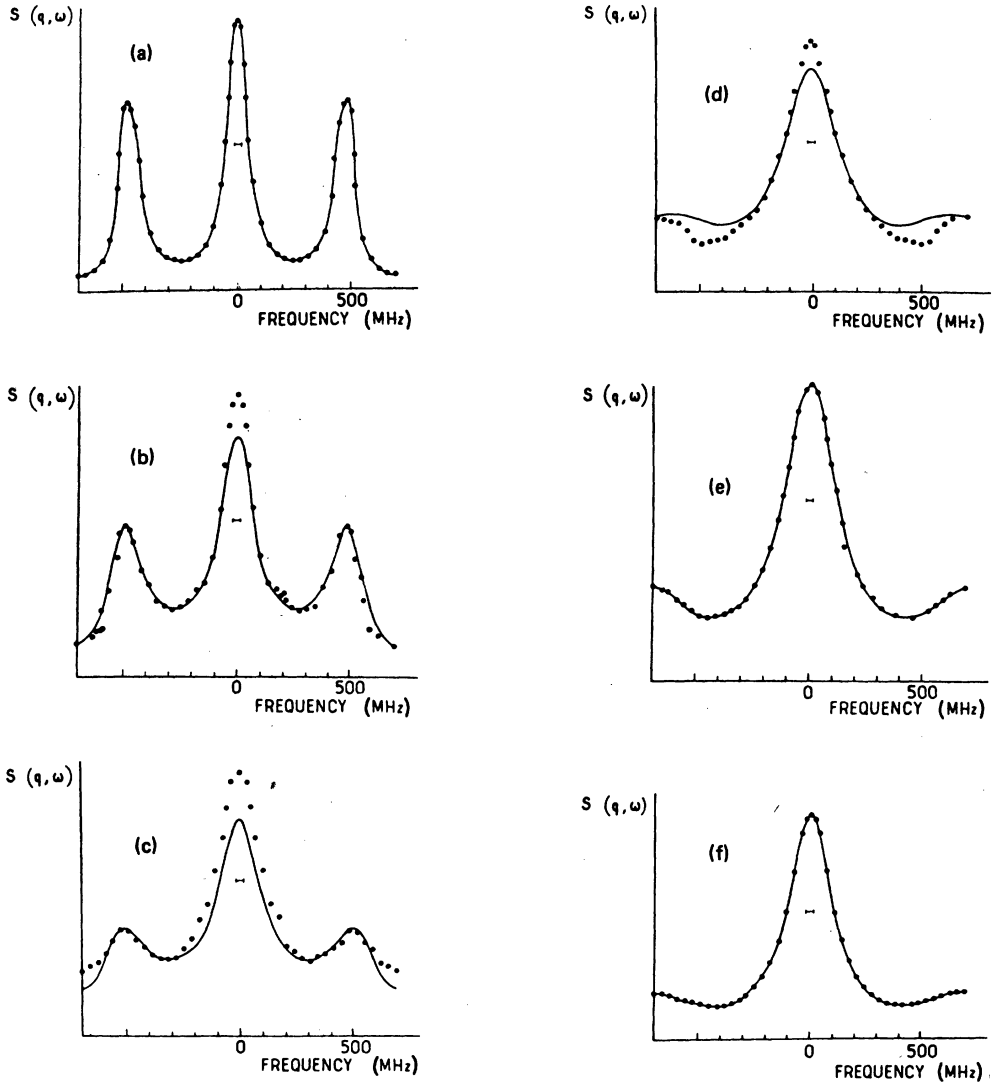

FIG. 6. Rayleigh-Brillouin spectra of He-Xe mixtures at $q = 1.727 \times 10^5$ cm^{-1}, $P_{Xe} = 7.32$ atm. (a) $P_{He} = 0$ atm; (b) $P_{He} = 1.59$ atm; (c) $P_{He} = 3.28$ atm; (d) $P_{He} = 7.14$ atm; (e) $P_{He} = 10.42$ atm; (f) $P_{He} = 13.14$ atm. See Fig. 3 for additional legend.

for an ideal gas mixture[10] [in our experiments, the weakness of nonideality corrections on $(\partial\mu/\partial c)_{P,T}$ allows us to discuss this point in terms of the simpler expression]:

$$\left(\frac{\partial\mu}{\partial c}\right)_{T,P} = \frac{1}{x(1-x)} \frac{[M_1 x + M_2(1-x)]^3}{(M_1 M_2)^2} RT_0$$

$$\simeq \frac{x^2}{1-x} \frac{M_1}{M_2} \frac{RT_0}{M_2},$$

where the second line is valid if x is not too small and $M_1/M_2 \gg 1$. Hence a large mass ratio M_1/M_2 produces an enhancement of the concentration-temperature coupling. Owing to this effect, it is possible to infer K_T from light-scattering experiments with an accuracy of better than 20%. This is illustrated in Fig. 10.

B. D_2-He and H_2-He binary mixtures

For the two cases the mass ratios M_1/M_2 are, respectively, 1 and 0.5 (label 2 refers to He). A new problem appears due to the fact that one of the components is diatomic: thermal equilibrium between the internal degrees of freedom of vibration and rotation and the translational motion requires a finite time when the translational temperature is suddenly modified. Extensive studies of dynamical behavior of H_2 and D_2 have been performed by May *et al.*,[17] and of H_2 by Cazabat *et al.*[18]

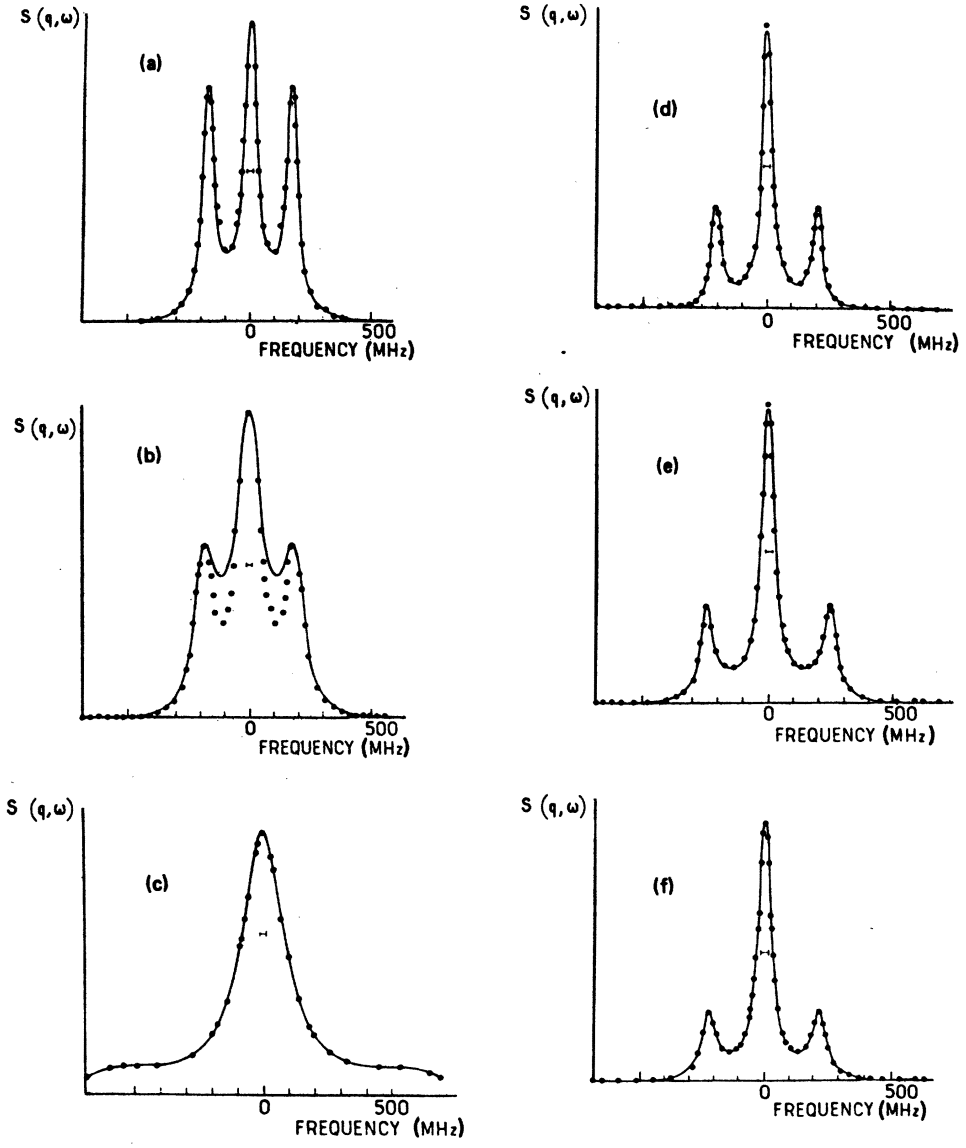

FIG. 7. Rayleigh-Brillouin spectra of He-Xe mixture at $q = 0.6316 \times 10^5$ cm^{-1}, $P_{Xe} = 2.66$ atm. (a) $P_{He} = 0$ atm; (b) $P_{He} = 1.11$ atm; (c) $P_{He} = 6.9$ atm; $P_{Xe} = 8.5$ atm; (d) $P_{He} = 4.0$ atm; (e) $P_{He} = 4.99$ atm; (f) $P_{He} = 6.8$ atm. See Fig. 3 for additional legend.

The vibrational and rotational temperatures are, respectively, $\sim\theta_{rot} = 85$ K, $\sim\theta_{vib} = 6130$ K for H_2; $\sim\theta_{rot} = 42$ K, $\sim\theta_{vib} = 4335$ K for D_2; at room temperature none of the excited vibrational levels are significantly populated and only the first rotational levels are populated. Desai and Kapral[19] have proposed a model for gases [translational hydrodynamics (TH)] in which thermalization occurs from relaxation and diffusion of the internal energy. For the mixtures there are two channels of relaxation: (i) H_2-H_2 (or D_2-D_2) collisions, (ii) He-H_2 (or He-D_2) collisions; the respective rates are $(Z_{11}\tau_{11})^{-1}$ and $(Z_{12}\tau_{12})^{-1}$ where the τ_{ij} are the mean collision times between particles i and j; rough values of the τ_{ij} are easily deduced from the corresponding Y_{ij}; Z_{ij} is the average number of collisions i-j which are necessary to thermalize the rotational degrees of freedom; Z_{11} has been evaluated by Cazabat[18] for H_2, values of Z_{12} are known for both He-H_2 and He-D_2 collisions from theory as well as experiments[20]: the values range around 100.

The value of the diffusion rate of internal energy is unknown for the H_2 (or D_2) molecules in the mixture, but since the self-diffusion coefficient of H_2 and the mutual diffusion coefficient of the mixture

TABLE III. Calculated values of the 4 Knudsen numbers Y_{ab} for He-H_2 and He-D_2 at different pressures, compositions, and 90° scattering. The last column (H) indicates that the spectrum can be accurately fitted to hydrodynamic theory.

Hydrogen-helium mixture							
P_{H_2} (atm)	P_{He} (atm)	Y_{H_2}	Y_{He}	$Y_{H_2\text{-}He}$	$Y_{He\text{-}H_2}$	X_{H_2}	
11.13	0	3.205	Pure	Hydrogen		1.0	H
11.13	1.22	3.205	0.221	0.651	8.43	0.895	H
11.13	3.65	3.205	0.689	1.954	8.43	0.751	H
11.13	9.19	3.205	1.671	4.923	8.43	0.529	H
11.13	27.17	3.205	4.94	14.56	8.43	0.29	H
11.13	37.14	3.205	6.752	19.906	8.43	0.233	H
Deuterium-helium mixture							
P_{D_2}	P_{He}	Y_{D_2}	Y_{He}	$Y_{D_2\text{-}He}$	$Y_{He\text{-}D_2}$	X_{D_2}	
11.22	0	3.225	Pure deuterium			1.0	H
11.22	1.82	3.225	0.325	1.129	6.96	0.861	H
11.22	2.72	3.225	0.493	1.685	6.96	0.805	H
11.22	6.35	3.225	1.153	3.937	6.96	0.639	H
11.22	24.78	3.225	4.501	15.37	6.96	0.312	H
11.22	53.28	3.225	9.69	33.05	6.96	0.174	H

He-H_2 are of the same order (12), we take $D_{12}q^2$ as an approximate value for the diffusion rate of internal energy. These three rates are to be compared with ω_B which is the characteristic frequency of the translational degrees of freedom. A crude calculation gives $\tau_{eff}\omega_B \simeq 10$ for both He-H_2 and He-D_2 in the range of pressure and composition studied. τ_{eff} is the effective relaxation time including three processes:

$$\tau_{eff}^{-1} = (\tau_{11}Z_{11})^{-1} + (\tau_{12}Z_{12})^{-1} + D_{12}q^2 .$$

This rough analysis shows that the Brillouin lines correspond to the high-frequency limit of the sound velocity, where exchanges of energy do not occur between rotational and translational degrees. The theoretical spectra have been calculated using hydrodynamic equations with thermodynamic and transport coefficients in which H_2 (or D_2) are taken as monoatomic.[23]

These are relevant conclusions from comparison between theoretical spectra and experimental data. First, good agreement with the hydrodynamic theory are obtained over the whole range of experiments even at low partial pressure of He, where $Y_{He\text{-}He}$ and $Y_{H_2\text{-}He}$ are <1. This observation seems to be in contradiction with the corresponding features on the He-Xe mixtures. However, this result may be understood from a simple argument. First, since masses and potential parameters (Table I) of He and H_2 (or D_2) are rather close to each other, addition of small amounts of He in H_2 (or D_2) should not disturb too much the dynamic behavior of the fluid because there are a number of relevant conclusions derived from comparison of theoretical spectra and experimental data. They are as follows. First, good agreement with the hydrodynamic theory is obtained over the whole range of experimental conditions, even at low partial pressure of He where Y_{He} and $Y_{H_2\text{-}He}$ are both less than unity. This is in sharp contrast with the corresponding observed features on the He-Xe mixtures. According to Boley and Yip[4] conditions for validity for hydrodynamic description are the following:

(i) All Y's greater than 1,
(ii) Y_a and $Y_{ba} > 1$, Y_b and $Y_{ab} < 1$,
(iii) Y_a, Y_{ab}, $Y_{ba} > 1$, $Y_b < 1$,

where a refers to H_2 or D_2, and b to He. Our observation, as shown in Figs. 8 and 9 and summarized in Table III, is in complete agreement with the above criteria.

We can also give a more physical argument. Since masses and potential parameters (see Table I) of He and H_2 (or D_2) are rather close to each other, addition of small amounts of He in H_2 (or D_2) gas should not disturb too much the dynamic behavior of the fluid because He-He, H_2-H_2 (or D_2-D_2), and He-H_2 (or He-D_2) collision cross sections are not significantly different. Therefore, the mixture could be described approximately by one Knudsen number which depends only on total density of the mixture. For our experimental conditions this Knudsen number is always greater than 1.

Another important point is that for both H_2-He and D_2-He mixtures, K_T and $(\partial\mu/\partial c)_{P,T}$ are both

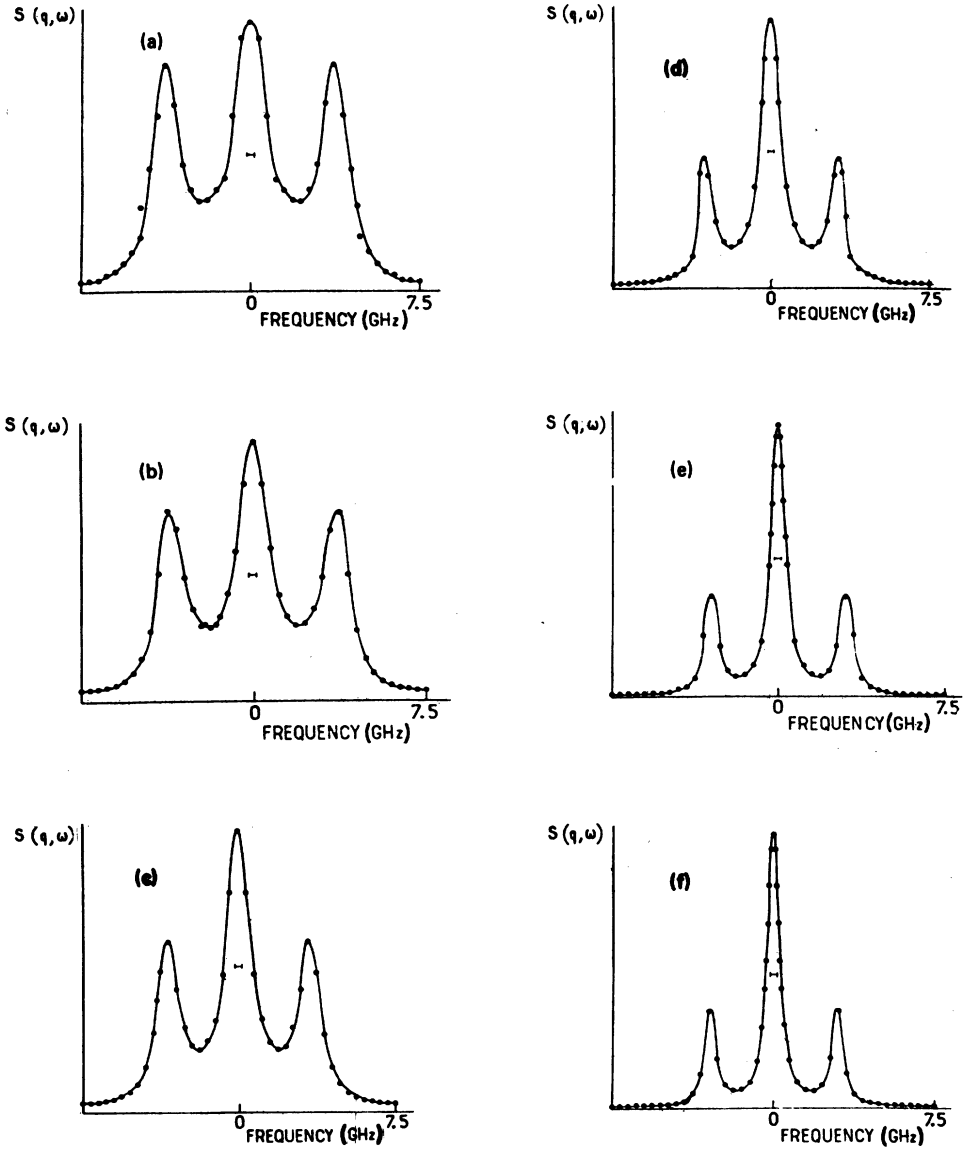

FIG. 8. Rayleigh-Brillouin spectra of the H_2-He mixture at $q = 1.727 \times 10^5$ cm^{-1}, $P_{H_2} = 11.13$ atm. (a) $P_{He} = 0$ atm; (b) $P_{He} = 1.22$ atm; (c) $P_{He} = 3.65$ atm; (d) $P_{He} = 9.19$ atm; (e) $P_{He} = 27.27$ atm; (f) $P_{He} = 34.14$ atm. See Fig. 3 for additional legend.

TABLE IV. Calculated parameters for the Xe-He mixture at $P_{Xe} = 5.97$ atm, $P_{He} = 3.8$ atm, scattering angle $\theta = 90°$; wavelength $\lambda = 5145$ Å; Γ_1; Γ_2; Γ_B are, respectively, the half-width at half maximum of the two central modes (integrated intensities α_1 and α_2) and of the Brillouin lines (frequency shift ω_B, integrated intensities $2B$, antisymmetric term B'). Γ_1, Γ_2, Γ_B, and ω_B are in MHz; $\alpha_1 + \alpha_2 + 2B = 100$.

	Γ_1	α_1	Γ_2	α_2	Γ_B	B	B'	ω_B
Hydrodynamic result	131	35.9	274	24.4	153	19.8	15.6	550
Best fit to the spectrum	101	58	1090.0	11.8	97.2	14.6	12.6	531

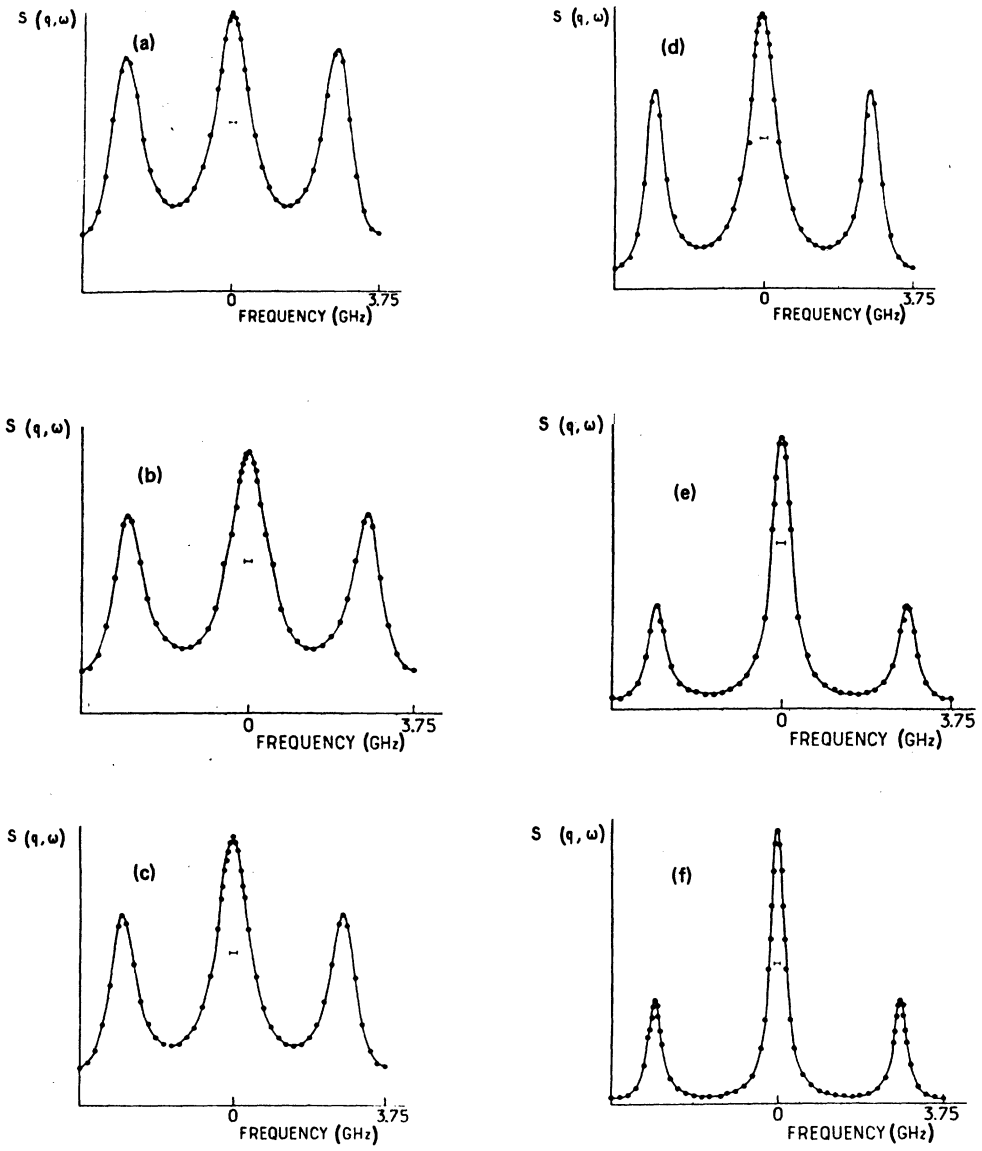

FIG. 9. Rayleigh-Brillouin spectra of He-D_2 mixture at $q = 1.727 \times 10^5$ cm^{-1}, $P_{D_2} = 11.22$ atm. (a) $P_{He} = 0$ atm; (b) $P_{He} = 1.82$ atm; (c) $P_{He} = 2.72$ atm; (d) $P_{He} = 6.35$ atm; (e) $P_{He} = 24.78$ atm; (f) $P_{He} = 53.28$ atm. See Fig. 3 for additional legend.

very small. Therefore, the coupling parameter δ between the two central modes is also small. Under this condition, one can assign the two central modes to be respectively a heat-diffusion mode and a concentration-diffusion mode. When concentration of He is small ($X_{He} < 0.2$) the intensity of the concentration-diffusion mode is very small and a precise measurement of width of the central line gives directly the thermal diffusivity D_T of the mixture.

TABLE V. Integrated intensities α_1 and α_2 when half-width at half maximum Γ_2 of the two central modes for $K_T = 0$ and $K_T = 0.321$ ($P_{Xe} = 5.97$ atm, $P_{He} = 9.17$ atm).

	α_1	Γ_1 (MHz)	α_2	Γ_2 (MHz)	B	B'	Γ_B (MHz)	ω_B (MHz)
$K_T = 0$	0.359	283	0.228	133	0.206	0.188	166	534
$K_T = 0.321$	0.10	180	0.679	146	0.11	0.121	223	686

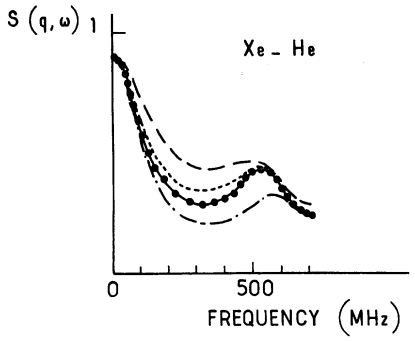

FIG. 10. Illustration of sensitivity of the Rayleigh-Brillouin spectra to variation of thermal diffusion coefficient K_T in the case of the He-Xe mixture. This spectrum is taken at $q=1.727\times10^5$ cm^{-1} for a mixture $Y_{Xe}=5.76$ and $Y_{He}=1.14$. The dotted line represents experimental data. The straight line represents hydrodynamic calculation with $K_T=0.321$. The dashed line represents hydrodynamic calculation with $\frac{1}{2}K_T$. The slashed line represents hydrodynamic calculation with $K_T=0$. The slash-dotted line represents hydrodynamic calculation with 5 K_T.

In the case of the D_2-He mixture, as the He concentration is increased frequencies of the two central modes approach each other and cross at a total pressure of 14.3 atm (with D_2 partial pressure at 11.2 atm, $X_{He}=0.23$). After the crossing the strength of the concentration-diffusion mode increases sharply and becomes greater than the thermal-diffusion mode. The intensity of the concentration-diffusion mode is 35% and the thermal-diffusion mode is 25% of the total intensity. This ratio stays roughly constant with further increases in He concentration. Consequently, light-scattering spectrum can be used to extract both D_T and D_{12} to about 5% accuracy.

VI. CONCLUSION

In this paper, new experimental results on three binary mixtures (Xe-He, H_2-He, D_2-He) have been reported. For the first mixture, good agreements have been obtained between experiment and hydrodynamic theory when (i) all 4 Knudsen numbers Y_{ab} are greater than 1; (ii) at low-He densities ($Y_{He}\ll1$, the 3 others $Y_{ij}>1$). In other situations kinetic effects are observed.

Occurrence of kinetic effects in Xe-He mixtures has been discussed by Clark[6] in regimes where Y_{Xe} is <1. Kinetic effects have also probably been observed by Baharuddin *et al.*[21] in Kr-He mixtures at moderate densities at back-scattering geometry. Their experiment corresponds to line D in Fig. 1. In the hydrodynamic regime, spectral shapes have been found to be sensitive to the value of the thermal-diffusion coefficient K_T and light scattering can be used as a tool for measuring this parameter. Since for the Maxwell model $K_T=0$, the usual assertion that the dynamic structure factor $S(q,\omega)$ of a binary gaseous mixture is insensitive to intermolecular potentials does not apply to the case of Xe-He mixtures where the mass ratio is very different from unity.

For He-H_2 and He-D_2 mixtures, a crude hydrodynamic model which assumes that H_2 and D_2 behave as monoatomic particles under a condition ($\omega_B\tau_{rot}\gg1$) satisfactorily fits the experimental results. Furthermore, in contrast to the Xe-He mixtures, dependence on K_T of the spectral shape is weak for both H_2-He and D_2-He mixtures. Therefore, at low densities the light-scattering spectra can be used to test the hydrodynamic limit of the two-component Boltzmann equations based on the Maxwell-model potential. Agreement with detailed mathematical analysis of such a model is found to be excellent.

ACKNOWLEDGMENTS

The authors are grateful to Dr. A. M. Cazabat for loan of high-pressure cells used in these experiments, and Professor Sidney Yip for helpful discussion with regard to the solution of two-component Boltzmann equations. S. H. Chen would like to acknowledge support from the National Science Foundation and NATO Research grant.

*Laboratoire Associe au C.N.R.S. No. 283.
[1](a) T. J. Greytak and G. B. Benedek, Phys. Rev. Lett. 17, 179 (1966); (b) A. M. Cazabat and P. Lallemand, J. Phys. C 33, 57 (1972); (c) N. A. Clark, Phys. Rev. A 12, 232 (1975); (d) J. E. Fookson, W. S. Gornall, and H. D. Cohen, J. Chem. Phys. 65, 350 (1976); (e) V. Ghaem-Maghami and A. D. May, Phys. Rev. A 22, 692 (1980); 22, 698 (1980).
[2]H. Bell *et al.*, Phys. Rev. A 11, 316 (1975); T. A. Postol and C. A. Pelizzari, *ibid.* 18, 2321 (1978).
[3]A. Sugawara, S. Yip, and L. Sirovich, Phys. Fluids 11, 925 (1968).
[4]C. B. Boley and S. Yip, Phys. Fluids 15, 1424 (1972); 15, 1433 (1972).
[5]W. S. Gornall and C. S. Wang, J. Phys. (Paris), C1 Suppl. 2-3, 33, 51 (1972).
[6]N. A. Clark, Phys. Rev. A 12, 2092 (1975).
[7]Q. H. Lao, P. E. Schoen, B. Chu, and D. A. Jackson, J. Chem. Phys. 64, 5013 (1976).
[8]C. Cohen, J. W. H. Sutherland, and J. M. Deutch, Phys. Chem. Liq. 2, 213 (1971).
[9]L. Letamendia, thesis, University of Bordeaux, 1979

(unpublished). This is an extension of work done earlier by W. B. Veldkamp, Ph.D. thesis, M. I. T., 1975 (unpublished).

[10]S. Chapman and T. G. Cowling, *The Mathematical Theory of Non-Uniform Gases* (Cambridge University Press, London, 1970); J. O. Hirschfelder, C. F. Curtiss, and B. B. Bird, *Molecular Theory of Gases and Liquids* (Wiley, New York, 1954).

[11]R. D. Mountain and J. M. Deutch, J. Chem. Phys. 50, 1103 (1969).

[12]H. Lekkerkerker and W. Laidlaw, Phys. Rev. A 5, 1604 (1972); 7, 1332 (1973).

[13]E. Thornton, Proc. Phys. Soc. London 76, 104 (1966).

[14]S. C. Saxena, Indian J. Phys. 31, 597 (1957).

[15]J. M. Saviron, C. M. Santamaria, J. A. Carrion, and J. C. Yarza, J. Chem. Phys. 63, 5318 (1975). Our K_T is denoted by α_T in this paper.

[16]S. R. de Groot and P. Mazur, *Non-Equilibrium Thermodynamics* (North-Holland, Amsterdam, 1969).

[17]H. Hubert and A. D. May, Can. J. Phys. 55, 23 (1977) and references therein.

[18]A. M. Longequeue-Cazabat and P. Lallemand, C. R. Acad. Sci. 269, 1173 (1969).

[19]R. C. Desai and R. Kapral, Phys. Rev. A 6, 2377 (1972).

[20]T. K. Bose, H. Zink, and A. Van Itterbeck, Phys. Rev. Lett. 19, 642 (1965); P. M. Agrawal and M. P. Kaksena, J. Phys. B 8, 1575 (1975).

[21]B. Y. Baharudin, P. E. Schoen, and D. A. Jackson, Phys. Lett. A42, 77 (1972).

[22]G. R. Staker and P. J. Dunlop, Chem. Phys. Lett. 42, 419 (1976).

[23]Transport coefficients of H_2-He and D_2-He mixtures are given by H. Cauwenberg and W. Van Dael, Physica (Utrecht) 54, 347 (1971); J. Kestin and J. Yata, J. Chem. Phys. 49, 4780 (1968); B. P. Mathur and W. W. Watson, *ibid.* 49, 5537 (1968).

[24]A. M. Cazabat, thesis, Paris University, 1976 (unpublished).